GMR
The Original

COMPARATIVE EVALUATION OF MATRIX ARCHITECTURE OF BIORESORBABLE SYNTHETIC GRAFT WITH AND WITHOUT I-PRF CONDITIONING USING SEM

Dr. Ankita Singh[1*], Dr. Ravikiran N.[2], Dr. Kratika Baldua Porwal[3], Dr. Vijeta Vyas[4], Dr. Alquama Rizvi[5], Dr. Neelam Kumar Das[6]

[1*]3rd year Post Graduate student, Department of Periodontology, Darshan Dental College and Hospital, Udaipur, Rajasthan, India. Email-Ankitasingh021@gmail.com , ORCID ID: 0009-0003-8957-6320
[2]Professor & Head, Department of Periodontology, Darshan Dental College and Hospital, Udaipur, Rajasthan, India E-mail: ravykiran@gmail.com, ORCID ID: 0000-0003-2238-4167
[3]Professor, Department of Periodontology, Darshan Dental College and Hospital, Udaipur, Rajasthan, India, Email-id-kritika261990@gmail.com, ORCID ID: 0009-0003-6259-8220
[4]Reader/Associate Professor, Department of Periodontology, Darshan Dental College and Hospital, Udaipur, Rajasthan, India, Email-id-vijetapanchu@gmail.com, ORCID ID: 0000-0002-9000-945X
[5]3rd year Post Graduate student, Department of Periodontology, Darshan Dental College and Hospital, Udaipur, Rajasthan, India, Email id - rizvialquama96@gmail.com, ORCID ID: 0009-0008-8148-5033
[6]3rd year Post Graduate student, Department of Periodontology, Darshan Dental College and Hospital, Udaipur, Rajasthan, India. Email: neelamkumardas2@gmail.com ORCID ID: 0009-0008-8143-1174

ABSTRACT:
Background: Alloplastic synthetic bone graft matrices offer excellent osteoconductive properties but lack intrinsic osteoinductive potential, prompting interest in combining them with autologous platelet concentrates like injectable platelet-rich fibrin (I-PRF) to enhance their biological activity. Henceforth the aim of our study was to evaluate and compare the matrix architecture of a bioresorbable synthetic graft matrix with and without I-PRF conditioning using scanning electron microscopy (SEM), in order to generate foundational evidence that may guide its clinical application in periodontal regenerative therapy.
Methods & Methodology: This in-vitro comparative study used six standardized samples (1×1 mm) of a bioresorbable synthetic graft matrix, divided into Group A (uncoated) and Group B (I-PRF conditioned, immersed for 20 minutes), followed by gold-sputtering and SEM-EDS analysis at 500x, 1000x, and 1500x magnifications to assess pore architecture, fiber compaction, surface roughness, and elemental composition.
Result: Group A exhibited a rough, highly porous, mineral-dominant surface (63.5% Ca, 34.5% P) with distinct interconnected macropores and granular crystalline morphology, while Group B showed a smoother, fibrin-coated surface with reduced pore visibility and a carbon/nitrogen-dominant elemental profile (61.9% C, 7.7% N) reflecting fibrin infiltration. I-PRF conditioning bridged and masked the macropores of Group A, creating a web-like fibrous network that reduced apparent surface roughness and porosity. EDS mapping confirmed a marked shift from mineral-based to organic-based elemental composition following I-PRF treatment, corroborating the SEM surface findings.
Conclusion: We conclude that, I-PRF conditioning meaningfully alters the pore architecture, fiber alignment, and surface composition of the bioresorbable synthetic graft matrix, imparting osteoinductive potential alongside its inherent osteoconductive properties.

KEYWORDS: Bioresorbable Synthetic Graft, Injectable Platelet-Rich Fibrin, Scanning Electron Microscopy, Matrix Architecture, Periodontal Regeneration

INTRODUCTION

Periodontal and alveolar bone defects resulting from periodontitis, trauma, or tooth extraction present a significant clinical challenge, as the body's intrinsic regenerative capacity is often insufficient to restore lost hard tissue architecture (Latimer et al., 2026 ; Marian, et al., 2024). Bone replacement grafts, broadly classified into autografts, allografts, xenografts, and alloplasts, have long been employed to fill osseous defects and provide a scaffold for new bone formation (Ferraz, 2023). Among these, alloplastic synthetic bone substitutes including calcium phosphate ceramics such as hydroxyapatite and β-tricalcium phosphate have gained widespread popularity due to their biocompatibility, predictable resorption, unlimited availability, and absence of donor-site morbidity or disease transmission risk associated with natural grafts (Fukuba et al., 2021). However, despite their favorable osteoconductive properties that support three-dimensional tissue ingrowth and cell attachment, purely synthetic alloplasts are generally devoid of intrinsic osteogenic or osteoinductive potential, often demonstrating inferior bone-forming ability compared to biologically active graft materials in

comparative studies (Ashfaq et al., 2024 ; Gapińska et al., 2026 ; Dhanavelu et al., 2025). To overcome this biological limitation, there has been growing interest in combining synthetic bone graft matrices with autologous platelet concentrates that can supplement the scaffold with bioactive growth factors and cellular components.

Platelet-rich fibrin (PRF), first developed by Choukroun et al. in 2001 as a second-generation platelet concentrate, revolutionized this field by offering a fibrin-based matrix enriched with platelets, leukocytes, and growth factors, prepared solely through centrifugation of autologous blood without the addition of anticoagulants or bovine thrombin (Dohan et al., 2006). Subsequent refinements led to injectable platelet-rich fibrin (I-PRF), a liquid formulation obtained through low-speed centrifugation that offers superior handling properties, allowing it to be injected or used to soak and condition solid graft materials before placement (Gollapudi et al., 2022). Moreover, the rationale for combining I-PRF with synthetic bone graft matrices lies in its ability to provide a three-dimensional fibrin scaffold loaded with growth factors that can enhance osteoblast proliferation, migration, differentiation, and angiogenesis, thereby imparting osteoinductive potential to an otherwise purely osteoconductive synthetic material. Previous morphological investigations using scanning electron microscopy have demonstrated that when I-PRF is combined with particulate hydroxyapatite, deproteinized bovine bone mineral, or other porous biomaterials, the flowable fibrin network infiltrates and coats the graft surface, filling macro- and micro-porosities and creating a cross-linked three-dimensional matrix around the mineral particles (Oliveira et al., 2024 ; Bueno et al., 2026). Such structural modifications at the microscopic level are considered central to the early events of bone healing, as the fibrin network can serve as a biological "glue" that stabilizes the graft while promoting cellular ingrowth (Noori, A et al., 2017 ; Bueno et al., 2026).

Despite this growing body of evidence supporting the biological rationale for I-PRF-graft combinations, there remains a paucity of direct morphological and elemental characterization comparing the surface architecture of specific bioresorbable synthetic graft matrices before and after I-PRF conditioning, particularly using combined SEM and energy dispersive spectroscopy (EDS) analysis. Understanding these micro-architectural changes which includes alterations in pore size, distribution, fiber compaction, and surface roughness, is utmost essential to elucidate how I-PRF conditioning may influence the graft's clinical handling, structural stability, and potential regenerative performance, since these microscopic surface characteristics directly govern the graft's cell attachment, vascular ingrowth, and osteogenic behavior in vivo. Therefore, the present study was undertaken to evaluate and compare the matrix architecture of a bioresorbable synthetic graft matrix with and without I-PRF conditioning using scanning electron microscopy, in order to generate foundational evidence that may guide its clinical application in periodontal regenerative therapy.

Objective of the Study

1. To evaluate the matrix architecture of bioresorbable synthetic graft matrix with I-PRF conditioning using SEM.
2. To evaluate the matrix architecture of bioresorbable synthetic graft matrix without I-PRF conditioning using SEM.
3. Comparison of bioresorbable synthetic graft matrix architecture with and without I-PRF conditioning using SEM.

METHODOLOGY

Study Design & Participants

This in-vitro comparative with no human tissue intervention study was done to investigate the effects of I-PRF on surface morphology, pore characteristics, and micro-architectural integrity of the bioresorbable synthetic bone graft material in the Department of Periodontology, Darshan Dental College and Hospital, Udaipur, in collaboration with the Central Research Laboratory, IIT Indore, for SEM evaluation, and all procedures were performed under stringent aseptic conditions in accordance with institutional ethical research protocols (Ref. No: DDCH-U/Perio/SEM/2025) in a single healthy volunteer who served as the venous blood donor for I-PRF preparation after obtaining voluntary informed consent.

Randomization and Study Groups

The bioresorbable synthetic graft matrix sheet (commercially available as Powerbone, 25×25×2 mm) as shown in figure 1,

Figure 1: Bone Graft

was used to prepare six standardised samples (1×1 mm) using a sterile BP blade (No. 11) under aseptic conditions as shown in figure 2.

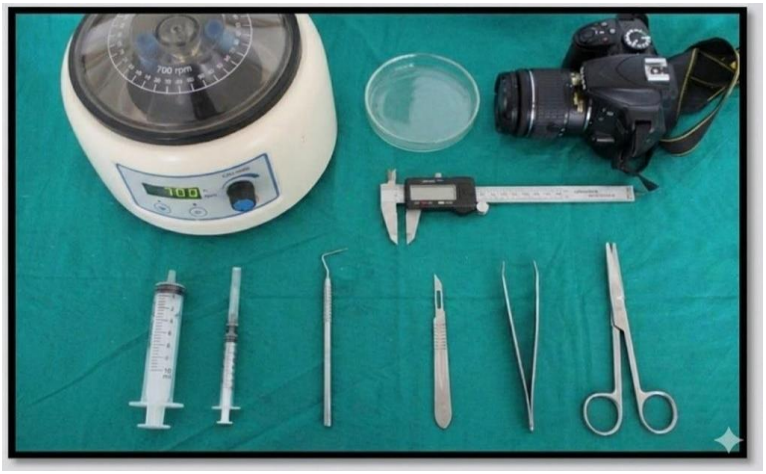

Figure 2 : Armamentarium

Further, the samples were divided equally into two groups (n = 6 per group) to ensure uniform dimensions for comparative evaluation wherein, group A was Bioresorbable synthetic graft matrix (BSGM) as control while on the other hand, group B was BSGM conditioned with I-PRF (Conditioned BSGM) as test group respectively.

Procedure

I-PRF was prepared following the low-speed centrifugation concept i.e., 9 mL of venous blood was collected from a healthy volunteer into sterile plain glass vacutainer tubes devoid of anticoagulant, followed by centrifugation at 700 rpm for 3 minutes to separate the upper orange I-PRF layer, which was aspirated and used within 2 minutes to preserve platelet vitality and growth factor stability. Group A samples were immersed in sterile saline solution to maintain dimensional consistency, while Group B samples were completely immersed in freshly prepared I-PRF for 20 minutes in sterile Petri dishes to allow uniform surface interaction; both groups were subsequently air-dried under laminar flow for 24 hours. For SEM preparation, each sample was mounted on aluminium specimen stubs using conductive carbon adhesive tape and sputter-coated with a thin gold layer (7–8 minutes) using a vacuum sputter coater to minimize specimen charging and improve resolution as shown in figure 3 &4.

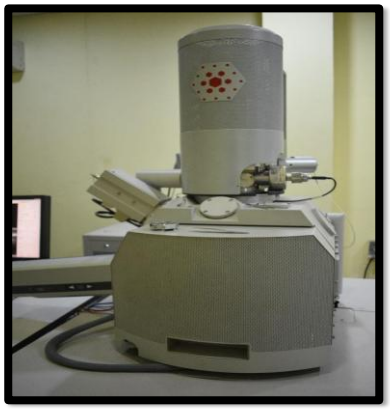

FIGURE 3 : SACNNING ELECTRON MICROSCOPE

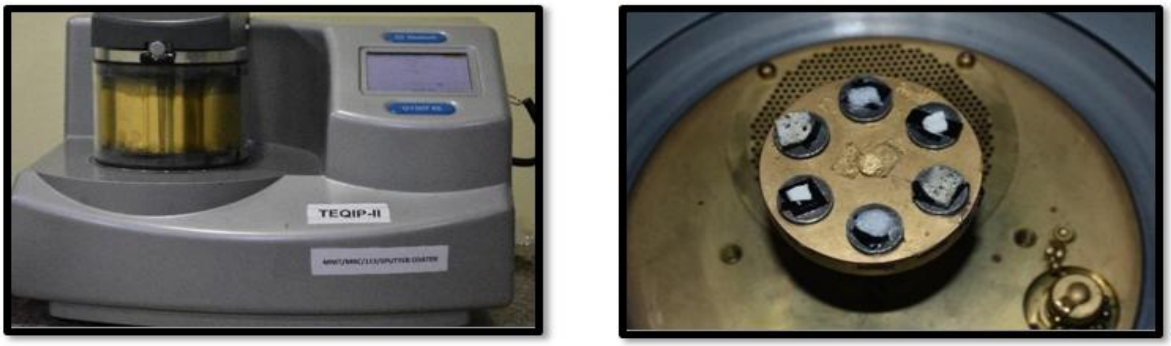

FIGURE 4 : GOLD COATING & SPUTTER COATER MACHINE

SEM analysis was performed at IIT Indore using a high-resolution Field Emission Scanning Electron Microscope integrated with Energy Dispersive Spectroscopy (EDS), with the electron beam accelerated under high vacuum to generate secondary, backscattered, and X-ray signals for three-dimensional surface topography reconstruction; each sample was examined at three magnifications (500×, 1000×, and 1500×).

Outcome Assessment

Micrographs from both groups were analysed and compared for surface porosity and pore arrangement, pore interconnectivity, fibre aggregation and matrix uniformity, and potential surface modifications following I-PRF conditioning. Qualitative evaluation focused on visual analysis of photomicrographs, while quantitative evaluation used calibrated SEM software to measure pore size (in micrometres, µm), fibre compaction and alignment, and porosity index and surface roughness between Group A and Group B.

Sample Size Estimation

Six standardised samples (1×1 mm) were prepared and divided equally into two groups (n = 6 per group; Group A and Group B) to ensure adequate and uniform representation for comparative SEM evaluation.

Statistical Analysis

Quantitative parameters like pore size, porosity index, and surface roughness, an appropriate approach would typically involve descriptive statistics (mean ± SD) for each group, followed by an independent samples t-test or Mann-Whitney U test (depending on data distribution/normality, often assessed via Shapiro-Wilk test) to compare Group A and Group B, with statistical significance set at $p < 0.05$, using software such as SPSS.

RESULT

TABLE 1 : EDS ELEMENTAL COMPOSITION FOR GROUP A

ELEMENT	WEIGTH%	ATOMIC%
Mg K	0.2	0.3
Si K	1.8	2.3
P K	34.5	40.0
Ca K	63.5	57.2

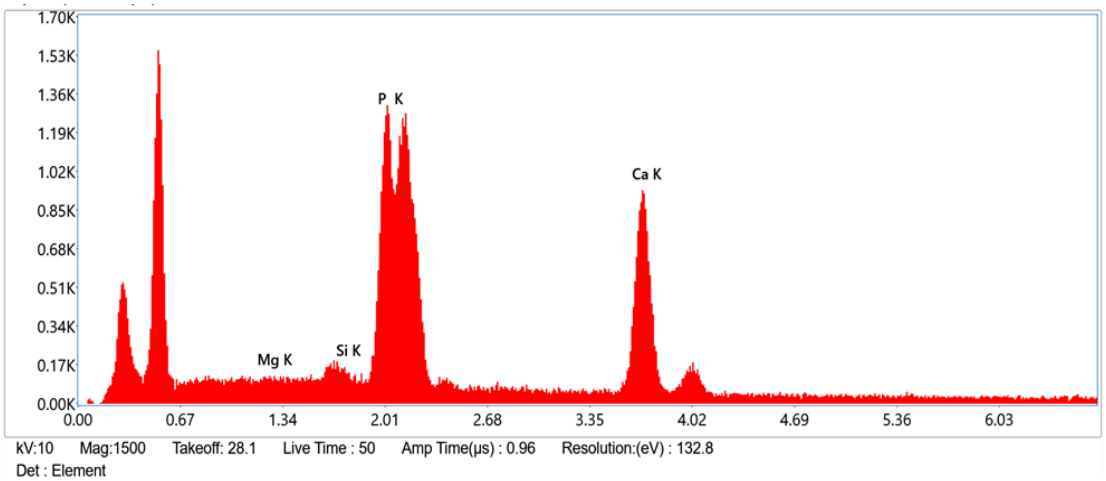

GRAPH 1: EDS ANALYSIS OF POWERBONE

Table 1 & graph 1 shows that, group A samples showed calcium as the predominant element (63.5% weight), followed by phosphorus (34.5%), confirming the material's composition as a silicate-substituted calcium phosphate-based bioresorbable graft. The high Ca/P ratio and trace magnesium and silica are consistent with a purely mineral, osteoconductive scaffold devoid of organic content.

TABLE 2 : EDS ELEMENTAL COMPOSITION FOR GROUP B

ELEMENT	WEIGHT%	ATOMIC%
CK	61.9	72.3
OK	19.4	17.0
NK	7.7	7.7
PK	1.8	0.8
Ca K	4.1	1.4
Nb L	5.1	0.8

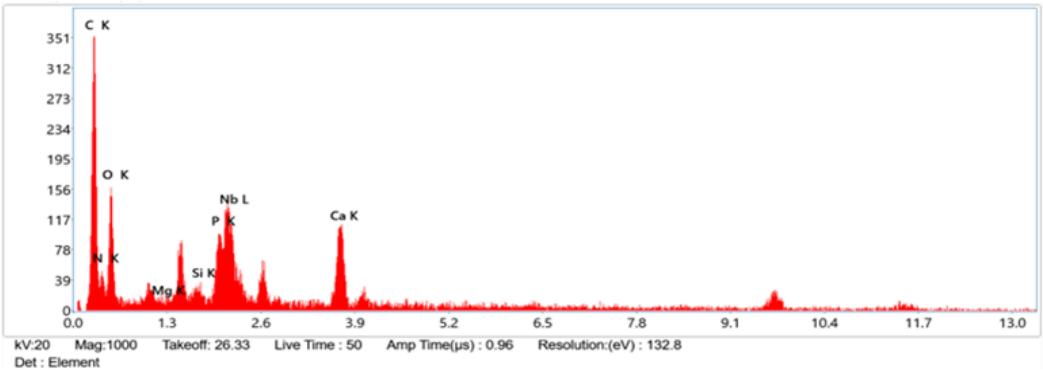

GRAPH 2 : EDS ANALYSIS OF POWERBONE CONDITIOMED WITH I-PRF

According to table 2 & graph 2 , we have found that, carbon emerged as the dominant element (61.9%), with a marked reduction in calcium (4.1%) and phosphorus (1.8%) compared to group A. The appearance of nitrogen, a specific marker of protein content, along with elevated carbon and oxygen, confirms that the fibrin matrix formed a thick organic layer that masked the underlying mineral graft surface.

TABLE 3 : COMPARATIVE ELEMENTAL ANALYSIS OF GROUP A & B

PROPERTY	GROUP A	GROUP B
Organic vs. mineral content	High mineral content (63.5% Ca, 34.5% P)	High organic content (61.9% C, 7.7% N)
Osteogenic properties	Osteoconductive (porous scaffold)	Osteoinductive potential (growth factors in I-PRF)
Calcium and phosphorus	Very high (~63% Ca, ~34% P) showed structural stability	Minimal detection (~4% Ca, ~1% P) thus masked by coating
Trace elements	Silica (Si), magnesium (Mg)	Niobium (Nb), nitrogen (N)
Surface masking	Absent (naked mineral surface)	Present (thick fibrin layer)

In table 3 we have found that, the elemental shift from a mineral-dominant profile (group A) to a carbon/nitrogen-dominant profile (group B) demonstrates that I-PRF successfully impregnated and coated the synthetic graft surface. This suggests Group A retains its intrinsic osteoconductive mineral scaffold, while Group B acquires additional osteoinductive biological potential at the expense of surface mineral exposure.

TABLE 4 : COMPARATIVE SURFACE CHARACTERISTICS OF GROUP A & B

SURFACE CHARACTERISTIC	GROUP A	GROUP B
Roughness	++	+
Pores	++	+

Pore shape	Irregular/granular	Fissured/cracked
Porosity	++	+
Mineral composition	Ca, P, Si	C, N, O
Organic content	Absent	Present

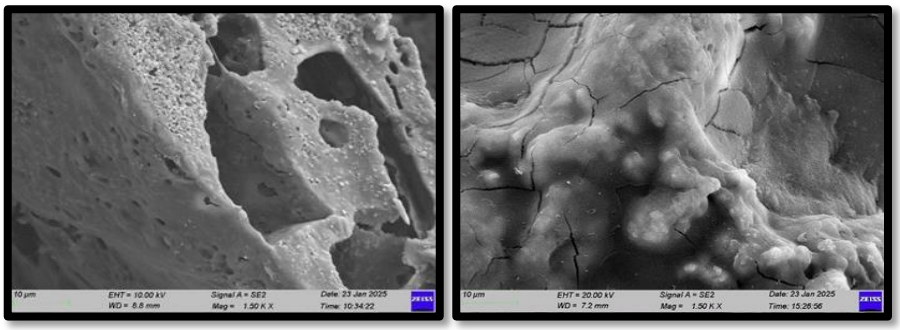

FIGURE 5 : COMPARATIVE SEM IMAGES OF POWERBONE (1500X) & POWERBONE CONDITIONED WITH I-PRF (1500X)

According to table 4 & figure 5 we have found that, group A exhibited a rougher, more porous, and irregularly granular topography, favorable for mechanical interlocking and cell attachment, whereas Group B showed reduced roughness and porosity with a fissured/cracked appearance, consistent with fibrin coating over the mineral surface. This confirms that I-PRF conditioning functions primarily as a surface modifier, converting an "open, mineral" architecture into a "coated, biologically active" one.

TABLE 5 : SEM QUALITATIVE COMPARISON WITH PORE, FIBER & SURFACE PARAMETERS

PARAMETER	GROUP A	GROUP B
Pore distribution	Open, heterogeneous macropores with distinct irregular borders	Macropores bridged/masked by fibrin, reduced open voids
Pore interconnectivity	High; deep, interconnected voids suggesting high permeability	Reduced; superficial gaps filled by fibrin coating
Fiber/matrix architecture	No intrinsic fibrous structure; granular, crystalline mineral aggregates	Dense fibrillar fibrin network draping over synthetic granules
Surface roughness	Marked roughness with sharp crystalline protrusions and deep crevices	Reduced roughness; smoother, more homogeneous surface
Visual porosity index	High, driven by jagged sintered particle geometry	Reduced "effective" porosity due to fibrin masking

500X	1000X	1500X

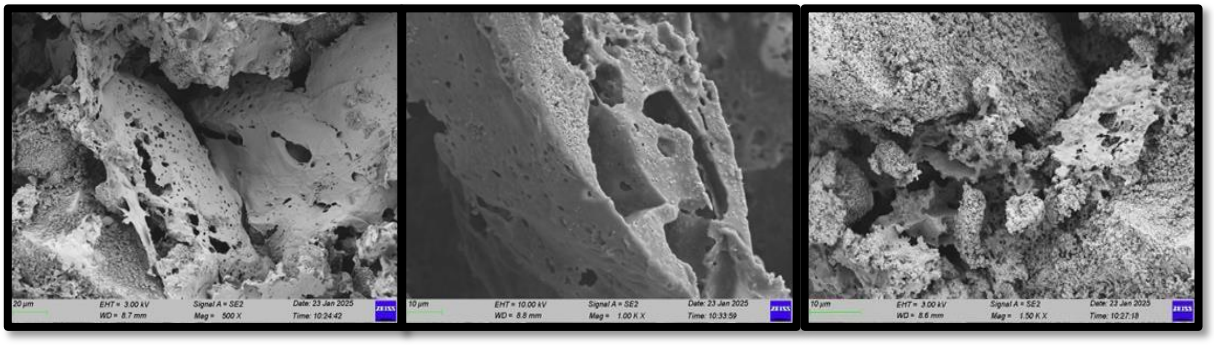

FIGURE 6 : SEM IMAGES OF POWERBONE (GROUP A)

500X	1000X	1500X

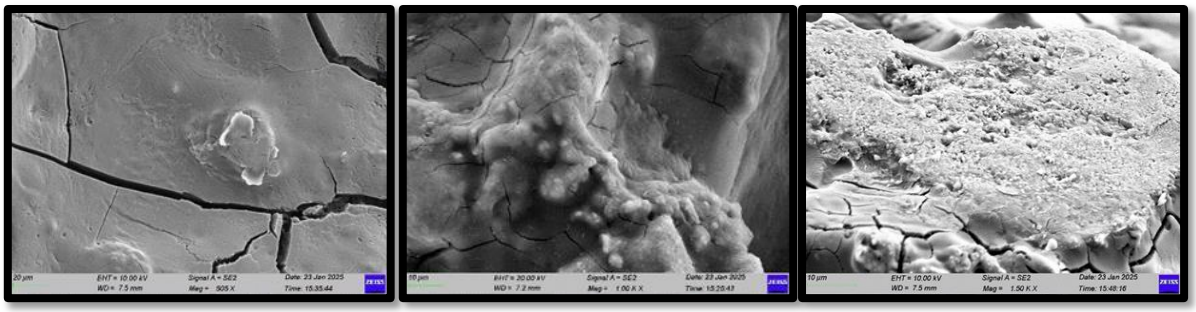

FIGURE 7 : SEM IMAGES OF POWERBONE CONDITIONED WITH I-PRF (GROUP B)

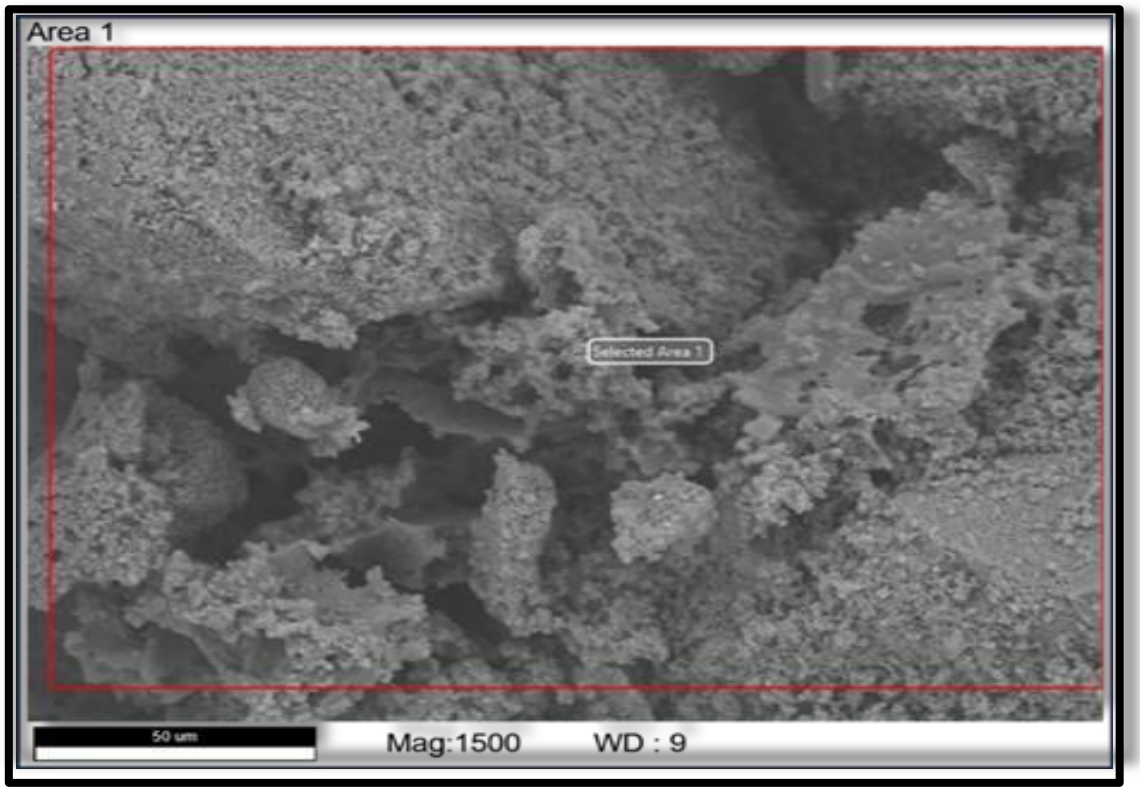

FIGURE 8 : SELECTED AREA FOR EDS MAPPING (POWERBONE)

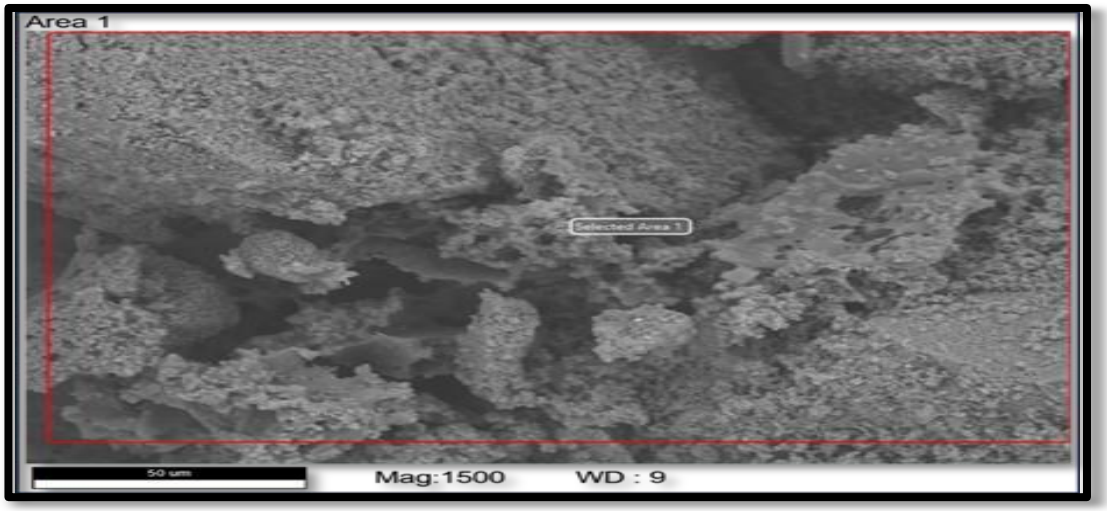

FIGURE 9 : SELECTED AREA FOR EDS MAPPING OF POWERBONE CONDITIONED WITH I-PRF

According to table 5, figure 6 to 9, we have found that, group A maintained a rigid, open, and rough mineral architecture ideal for fluid uptake and mechanical cell interlocking, while Group B demonstrated a biologically integrated, smoother surface where the I-PRF fibrin network occupied pore spaces and bound granules together. This qualitative shift from a "rough and jagged" to a "smooth and coated" topography supports the hypothesis that I-PRF conditioning enhances the graft's biological functionalization without compromising its underlying structural framework, potentially improving initial cellular attachment and soft-tissue response.

DISCUSSION

The present in-vitro study demonstrated distinct morphological and elemental differences between the uncoated bioresorbable synthetic graft matrix (Group A) and the I-PRF conditioned graft (Group B) using SEM and EDS analysis. group A exhibited a highly porous, open, and irregular crystalline architecture rich in calcium, phosphorus, and silica, whereas group B showed a fibrin-coated surface with reduced apparent porosity, dominated by carbon and nitrogen signals. These findings align closely with a study, where authors reported that when injectable PRF was combined with particulate hydroxyapatite and deproteinized bovine bone mineral granules, the fibrin network entirely embedded the biomaterial particles, filling the porous spaces and coating rough surfaces, similar to the "bridging" and pore-masking effect observed in our group B samples (Oliveira et al., 2024). Similarly, a review done on the feasibility of I-PRF for bone tissue engineering emphasized that I-PRF's flowable fibrin matrix readily infiltrates graft porosities and cross-links around particulate biomaterials, supporting our SEM observation of a continuous, web-like fibrin layer draping over the granular Powerbone surface (Farshidfar et al., 2022).

Moreover, our EDS findings, showing a shift from a mineral-dominant profile (63.5% Ca, 34.5% P) in group A to a carbon/nitrogen-dominant profile (61.9% C, 7.7% N) in group B, are consistent with the morphological analysis where, authors used SEM-EDX to confirm that PRF-coated bone substitutes displayed a marked reduction in detectable calcium and phosphorus signals due to the overlying organic fibrin layer, despite the mineral scaffold remaining structurally intact beneath (Liu, Y et al., 2019). This masking phenomenon has also been documented in studies combining PRF with recombinant collagen-based porous particles, where SEM revealed that fibrin fiber thickness and cross-link density created a mesh-like arrangement over the underlying scaffold (Tsukioka et al., 2019 ; Oliveira et al., 2024 ; Karimi et al., 2022) which was comparable to the "blanket effect" that we observed. In contrast to our qualitative pore-masking findings, some in vitro literature notes found that despite surface coating, the intrinsic mesh architecture of PRF itself retains an "irregular grid-like arrangement of loose fibers and pores," suggesting that the biological layer does not entirely eliminate porosity but rather redistributes and modifies its expression at the microscopic level (Dohan et al., 2006 ; Saluja et al., 2011 ; Zuleika et al., 2024).

The reduced surface roughness observed in group B, attributable to the fibrin's smoothing effect over jagged synthetic crystalline protrusions, parallels observations in PCL-hydroxyapatite scaffold studies, where PRF incorporation was associated with increased hydrophilicity and altered surface texture compared to uncoated scaffolds, correlating with enhanced cell attachment and proliferation in subsequent cytocompatibility assays (Yal et al., 2022 ; Qin et al., 2022). This was clinically relevant because a study demonstrated that I-PRF addition to allogeneic and xenogeneic bone grafts enhances osteoblast viability, proliferation, migration, and attachment (Farshidfar et al., 2022), potentially explaining why the structurally "rougher" group A surface favors initial mechanical interlocking while the "smoother, coated" group B surface may better support early biological cell migration, as proposed in our comparative evaluation. However, in contrast to our study results another research reported that despite surface coating effects, PRF-covered scaffolds like PCL-mesh still permitted extensive osteoblast colonization within lattice gaps, suggesting that fibrin coating does not necessarily impede but may instead guide cellular ingrowth pathways (Al-Maawi et al., 2021). In addition to above, our purely elemental and morphological findings should be interpreted cautiously against functional outcome data, since a not more recent systematic review and meta-analysis found that PRF alone generally produces less new bone volume than conventional graft materials in larger defects, despite favorable surface and biological properties observed at the microscopic level, underscoring the distinction between morphological compatibility and in vivo osteogenic efficacy (Alfaraj, et al., 2025 ; Ieviņa & Dubņika 2024). This is further supported by a study where reserachers found that combining PRF with a synthetic ceramic graft significantly increased new bone formation and density compared to PRF alone (Nacopoulos et al., 2014), reinforcing that our observed "bio-functionalized" surface architecture in group B may translate into synergistic regenerative benefits when the mineral scaffold and organic fibrin network act in combination rather than as substitutes for one another.

Henceforth, our SEM-EDS results corroborate existing literature demonstrating that I-PRF conditioning of synthetic bone grafts alters surface topography, elemental composition, and porosity patterns, transforming an inert mineral scaffold into a bio-functionalized composite, though further in vivo and cellular studies would be needed to correlate these structural changes with actual osteogenic and osteoinductive performance.

CONCLUSION

This in-vitro comparative SEM-EDS study evaluated the matrix architecture of a bioresorbable synthetic graft matrix with and without I-PRF conditioning, revealing distinct structural and elemental differences between the

two groups. The uncoated matrix (Group A) displayed a rough, highly porous, mineral-rich surface dominated by calcium, phosphorus, and silica, consistent with an osteoconductive scaffold offering open, interconnected pores suited for fluid uptake and mechanical cell interlocking. Conversely, I-PRF conditioning (Group B) produced a smoother, biologically coated surface in which the fibrin network infiltrated and partially masked the graft's pores, shifting the elemental composition toward a carbon- and nitrogen-dominant profile reflective of proteinaceous fibrin content. This shift from a purely granular, mineral-based structure to a fiber-reinforced, bio-functionalized composite suggests that I-PRF acts as a surface modifier that enhances the graft's biological potential without disrupting its underlying architectural integrity. Within the limitations of this in-vitro analysis, it may be concluded that I-PRF conditioning meaningfully alters the pore distribution, fiber alignment, and surface roughness of the bioresorbable synthetic graft matrix, imparting osteoinductive potential in addition to its inherent osteoconductive properties. These observations support the combined use of synthetic bone substitutes with autologous I-PRF in regenerative periodontal therapy, warranting further in vivo and cellular validation of their clinical translational benefit.

REFERENCES

1. Latimer, J., Wu, D. T., Yilmaz, B. T., Cha, J. K., Gouveia, Z., Yao, Y., & Giannobile, W. (2026). Biological principles for success in alveolar bone, soft tissue, and periodontal regeneration. Journal of Periodontal Research.
2. Marian, D., Toro, G., D'Amico, G., Trotta, M. C., D'Amico, M., Petre, A., ... & Fratila, A. (2024). Challenges and innovations in alveolar bone regeneration: a narrative review on materials, techniques, clinical outcomes, and future directions. Medicina, 61(1), 20.
3. Ferraz, M. P. (2023). Bone grafts in dental medicine: an overview of autografts, allografts and synthetic materials. Materials, 16(11), 4117.
4. Fukuba, S., Okada, M., Nohara, K., & Iwata, T. (2021). Alloplastic Bone Substitutes for Periodontal and Bone Regeneration in Dentistry: Current Status and Prospects. Materials (Basel, Switzerland), 14(5), 1096.
5. Ashfaq, R., Kovács, A., Berkó, S., & Budai-Szűcs, M. (2024). Developments in alloplastic bone grafts and barrier membrane biomaterials for periodontal guided tissue and bone regeneration therapy. International journal of molecular sciences, 25(14), 7746.
6. Gapińska, N., Śmielecki, M., & Krasny, K. (2026). Comparative Analysis of Bone Remodeling Dynamics and Bone Vitality Following Standard Bone Augmentation Procedures: A Review. Journal of Functional Biomaterials, 17(8), 398.
7. Dhanavelu, P., Nandagopal, K. G., Ganesh, N. S., Athira, K. S., Quadri, A., & Francis, M. (2025). In Vitro Evaluation of the Osteogenic Potential of Different Bone Graft Materials in Oral Surgery. Journal of Pharmacy & Bioallied Sciences, 17(Suppl 3), S2656.
8. Dohan, D. M., Choukroun, J., Diss, A., Dohan, S. L., Dohan, A. J., Mouhyi, J., & Gogly, B. (2006). Platelet-rich fibrin (PRF): a second-generation platelet concentrate. Part II: platelet-related biologic features. Oral Surgery, Oral Medicine, Oral Pathology, Oral Radiology, and Endodontology, 101(3), e45-e50.
9. Gollapudi, M., Bajaj, P., & Oza, R. R. (2022). Injectable platelet-rich fibrin-a revolution in periodontal regeneration. Cureus, 14(8).
10. Oliveira, M. N., Varela, H. A., Nascimento, R. M., Sahoo, N., Carvalho, O., Henriques, B., & Souza, J. C. (2024). Injectable platelet-rich fibrin in contact with bone substitutes, porous zirconia, or laser-textured implant surfaces: a detailed morphological analysis. Biomedical Materials & Devices, 2(1), 415-426.
11. Bueno, L. M. M., Dos Santos, C. P. C., Cruel, P. T. E., Romanini, G., Padula, L. R. C., dos Santos Oliveira, C. R., ... & Buchaim, R. L. (2026). Bone-Healing Enhancement Using Particulate Biomaterials and Fibrin-Based Compounds: A Narrative Literature Review of Evidence in Animal Models. Materials, 19(2), 224.
12. Noori, A., Ashrafi, S. J., Vaez-Ghaemi, R., Hatamian-Zaremi, A., & Webster, T. J. (2017). A review of fibrin and fibrin composites for bone tissue engineering. International journal of nanomedicine, 4937-4961.
13. Farshidfar, N., Amiri, M. A., Jafarpour, D., Hamedani, S., Niknezhad, S. V., & Tayebi, L. (2022). The feasibility of injectable PRF (I-PRF) for bone tissue engineering and its application in oral and maxillofacial reconstruction: From bench to chairside. Biomaterials advances, 134, 112557.
14. Liu, Y., Sun, X., Yu, J., Wang, J., Zhai, P., Chen, S., ... & Zhou, Y. (2019). Platelet-rich fibrin as a bone graft material in oral and maxillofacial bone regeneration: classification and summary for better application. BioMed research international, 2019(1), 3295756.
15. Tsukioka, T., Hiratsuka, T., Nakamura, M., Watanabe, T., Kitamura, Y., Isobe, K., ... & Kawase, T. (2019). An on-site preparable, novel bone-grafting complex consisting of human platelet-rich fibrin and porous particles made of a recombinant collagen-like protein. Journal of Biomedical Materials Research Part B: Applied Biomaterials, 107(5), 1420-1430.
16. Karimi, F., Biazar, E., Heidari-Keshel, S., Pourjabbar, B., Khataminezhad, M. R., Shirinbakhsh, S., & Zolfaghari-Moghaddam, S. Y. (2022). Platelet-rich fibrin (PRF) gel modified by a carbodiimide crosslinker for tissue regeneration. RSC advances, 12(21), 13472-13479.
17. Saluja, H., Dehane, V., & Mahindra, U. (2011). Platelet-Rich fibrin: A second generation platelet concentrate and a new friend of oral and maxillofacial surgeons. Annals of maxillofacial surgery, 1(1), 53.

18. Zuleika, P., Saleh, I., Murti, K., Liberty, I. A., & Surono, A. (2024). Platelet-rich fibrin: A systematic review of its action. Journal of Nature and Science of Medicine, 7(4), 242-252.
19. Yal, B. S., Nourani, H., & KAZEMI, M. H. (2022). Fabrication of platelet-rich fibrin-coated polycaprolactone/hydroxyapatite (PCL-HA/PRF) 3D printed scaffolds for bone tissue engineering.
20. Qin, X., Wu, Y., Liu, S., Yang, L., Yuan, H., Cai, S., ... & Yu, C. (2022). Surface modification of polycaprolactone scaffold with improved biocompatibility and controlled growth factor release for enhanced stem cell differentiation. Frontiers in Bioengineering and Biotechnology, 9, 802311.
21. Al-Maawi, S., Dohle, E., Lim, J., Weigl, P., Teoh, S. H., Sader, R., & Ghanaati, S. (2021). Biologization of Pcl-mesh using platelet rich fibrin (Prf) enhances its regenerative potential in vitro. International journal of molecular sciences, 22(4), 2159.
22. Alfaraj, T. M. A., Alruwaili, B. M., Alnasser, R. F., Alqahtani, S. H., Alrajhi, T. N., Alqahtani, M. A., ... & Alhashim, N. S. (2025). Platelet-Rich Fibrin as a true bone graft substitute: a systematic review and meta-analysis of its osteogenic potential in dental and maxillofacial surgery. Cureus, 17(7), e89082.
23. Ieviņa, L., & Dubņika, A. (2024). Navigating the combinations of platelet-rich fibrin with biomaterials used in maxillofacial surgery. Frontiers in Bioengineering and Biotechnology, 12, 1465019.
24. Nacopoulos, C., Dontas, I., Lelovas, P., Galanos, A., Vesalas, A. M., Raptou, P., ... & Papaioannou, N. (2014). Enhancement of bone regeneration with the combination of platelet-rich fibrin and synthetic graft. Journasl of Craniofacial Surgery, 25(6), 2164-2168.